An evaluation and regulation method for stereoscopic spatial connectivity of a wetland system based on hydrological change: A case study of the Heilongjiang River Basin in China

Qin Yang[1], Peng Hu[2], Jianhua Wang[3], Qinghui Zeng[3], zefan yang[2], Huan Liu[3], and Yiyang Dong[1]

[1]Tsinghua University
[2]IWHR
[3]China Institute of Water Resources and Hydropower Research

May 18, 2020

Abstract

The weakened connectivity of wetland systems is the key factor leading to the destruction, degradation, and disappearance of wetlands. The study of the change of wetland system connectivity enables understanding the hydrological process in wetland system and providing significant support for the study of ecological water demand. However, research on the connectivity of wetland systems has primarily focused on the intuitive connectivity in terms of hydrology and geomorphology in recent years, while the impact of wetland systems on habitat has been ignored. In this study, an innovative method was applied to evaluate and regulate the stereoscopic spatial connectivity (SSC) of the wetland system in the Heilongjiang River Basin in China (HRBC). In this method, the water requirements of typical organisms in the region were considered, and the hydrological trend in the wetland system as well as the health conditions of the SSC were analyzed using remote sensing image. A regulation mode for improving the stereoscopic spatial connectivity index (SSCI) was proposed. The results revealed that over the past 35 years, the wetland system in the study area shrank significantly, with the SSCI decreasing from 41.30% in 1980 to 35.08% in 2015. By comparing the correlation among temperature, precipitation, agricultural land, construction land, and the wetland system during the same period, it was proven that human activity is the major driving force behind the observed wetland system shrinkage. Subsequently, the key protected areas required to maintain the SSC of the wetland system were clarified, and the key recovery areas were determined according to the three scenarios of 'high–medium–low' feasibility, which greatly improved the SSCI and generalization route (GR) after regulation. In general, the proposed SSC evaluation methods can fully reflect the ecohydrological process of wetland systems. The methods also scientifically quantify the significant effects of the regulation mode, which has certain relevance for the evaluation and regulation of wetland systems in other regions.

1. Introduction

Abbreviations: CA, connected area; DEM, digital elevation model; EWS, effective water surface; GIS, geographic information system; GR, generalization route; HA, habitat area; HRBC, Heilongjiang River Basin in China; KRA, key recovery area; MA, migration area; RCA, restored connected area; SRTM, Shuttle Radar Topography Mission; SSC, stereoscopic spatial connectivity; SSCI, stereoscopic spatial connectivity index.

The wetland is one of the most important natural systems. Wetlands, along with forests and oceans, constitute the world's three major ecosystems (Costanza et al., 1997). The wetland system is an important part of the natural ecological environment. It plays an important role in conserving water sources, purifying water quality, regulating storage and drought resistance, maintaining biodiversity, etc., especially in providing important ecological service functions in the hydrological process, all of which support the sustainable development of human economic society and living environments (Zhang et al., 2018). Under the combined effects of global climate change and human activity, however, the water cycle in the river basin and its associated physical, chemical, and biological processes have undergone profound changes, leading to changes in the hydrology of wetlands, water resource shortages, water quality deterioration, area shrinkage, and functional degradation (Acreman et al., 2007; Dong and Zhang, 2013; Zedler, 2003; Zedler and Kercher, 2005; Zhang et al., 2008). According to the Intergovernmental Science-Policy Platform on Biodiversity and Ecosystem Services (IPBES), 87% of the world's wetlands have been lost over the past 300 years and 54% since 1900, making it one of the most severely damaged ecosystems in the world. Since the 1950s, the loss of wetlands in tropical and subtropical regions, where agriculture is the main cause, has accelerated. In Asia, approximately 5,000 km^2 of wetland area disappears every year due to human activities, such as dam construction and agriculture, and up to 50% of the remaining wetlands are threatened and degraded (Acreman et al., 2007). The results of the Second China Wetland Data Survey (2009–2013) revealed that the total wetland area in China is 5.4×10^7 hm^2, and the overall proportion of wetlands in China during this period was 5.6%, which was less than the world average of 8.6%. The total area of natural wetlands is 46.67 million hm^2, accounting for 87.1% of the total wetland area. Compared with the first survey in 2003, the area of natural wetlands decreased by 3.38 million hm^2, a loss rate of 9.3%. In addition, approximately 69.3% of wetlands are threatened by overgrazing, pollution, and reclamation, threats that exert a great impact on the protection of the ecological environment and the development of economy and society (Niu et al., 2012). Therefore, the wetland is an important strategic ecological resource. The destruction, degradation, and disappearance of wetland systems have caused major problems in the aquatic ecology and hydrological processes of wetlands.

Most of the transfer processes of material, energy, and information flow in wetland systems are related to connectivity. The weakened connectivity of wetland systems is the key factor leading to the destruction, degradation, and disappearance of wetlands. In the usual sense, connectivity includes 3 facets: geomorphology, hydrology, and biological processes. The connectivity of geomorphic systems is defined as the efficiency of material transfer between system components (Wohl et al., 2019), where the material can be water, sediment, nutrients, and so on, and the system components can be rivers, wetlands, or watersheds. The connectivity of hydrological systems refers to the connectivity of water transfer between components of the system. The hydrological connectivity of wetlands determines their soil type, water chemistry, and vegetation structure (Cook and Hauer, 2007), which governs their ecology and persistence (Ferone and Devito, 2004). Previous research on the hydrological connectivity of wetlands has focused on the interconnections between wetlands and adjacent water bodies, such as rivers, streams, and other wetlands, in order to grasp the temporal and spatial (dynamic) connection structure of wetlands relative to their watersheds (Ameli and Creed, 2017; Evenson et al., 2015; Jaramillo et al., 2018; Karim et al., 2012; Karim et al., 2014; Karim et al., 2016; Leibowitz and Vining, 2003; McDonough et al., 2015). Some researchers have also proposed the vertical connectivity, horizontal connectivity, and temporal connectivity of wetland water systems. They utilized a variety of indicators to comprehensively quantify the connectivity of the systems, providing a basis for identifying areas of aquatic biota that are vulnerable to interference using appropriate scenario models (Januchowski-Hartley et al., 2013; Poff and Zimmerman, 2010; Richter et al., 1996; Rivers-Moore et al., 2016). This brief literature overview indicates that the current research on wetland connectivity has primarily focused on two-dimensional plane scale connectivity. For a large number of migratory birds that are important protection targets of wetlands, however, their requirements for wetland connectivity are better reflected in the process of habitation and migration. For example, an appropriate distance between wetlands is required to meet the needs of short stays and rest intervals during the flight of migratory birds and for flying from one habitat to another. This kind of connectivity requirement breaks through the two-dimensional plane characteristics of the existing wetland connectivity evaluation, and is referred to as the stereoscopic spatial connectivity (SSC) of wetlands in this manuscript.

This study had the following objectives: (1) Establish an innovative theoretical framework for the evaluation and regulation of the SSC of wetland systems and propose a calculation method for the stereoscopic spatial connectivity index (SSCI). (2) Interpret the land use types in the Heilongjiang River Basin in China (HRBC) using remote sensing, and screen the wetland systems suitable for the habitat of typical migratory birds (i.e., red-crowned cranes). Then analyze and discuss the evolutionary trend of the wetland system and explore its important driving factors. (3) Calculate the SSCI of typical years and evaluate the SSC in wetland systems. (4) Develop a multi-scenario regulation scheme for the comparative analysis of the connectivity effect after regulation. The method of evaluating and regulating the SSC of wetland systems proposed in this study not only provides valuable support for the protection, restoration, and sustainable management of the wetland system in the HRBC, but also has important significance for other wetland systems with typical migratory bird protection requirements.

2. Study area and datasets

2.1. Study area

Fig. 1 . (a) Map of study area and (b) Red-crowned crane's migration route.

The Heilongjiang River (also known as the Amur) is the largest river in Northeast Asia. It is located between 47°40'–53deg34'N and 121deg28'–141deg20'E. Its river basin spans China, Mongolia, and Russia, with an area of more than 1.8 million km^2. The study area of this investigation was the Heilongjiang Basin in China (Fig. 1a). In this river basin, the Heilongjiang is the main stream, while the main tributaries include the Songhua River, the Wusuli River, and the Nenjiang River. The length of Heilongjiang River in China is approximately 2,320 km, the watershed area is 0.91 million km^2, and the areas of the mountains and the plains are almost equal. The lowest monthly average temperature in the area is below -30degC in January, while the highest is 16degC–18degC in July. The annual average precipitation is 579.1 mm. Within the study area, the Daxing'an Mountains are situated to the west, the Changbai Mountains to the east, and the Xiaoxing'an Mountains to the north. The valley is surrounded by mountains on three sides, and contains the Sanjiang Plain and Songnen Plain.

The HRBC is located in humid, semi-humid, and semi-arid climate zones. There are numerous types of wetlands in this basin, including 12 types of freshwater wetlands. The rivers in the study area are mostly plain rivers with flat terrain, which is not conducive to drainage. Therefore, the rivers overflow into swamp wetlands consisting of scattered and diffuse marshes, accounting for 66.2% of the total wetland area. Based on the characteristics of wetland distribution, the wetland can be divided into five areas: the Daxing'anling Wetland, the Xiaoxing'anling Wetland, the Changbai Mountain Wetland, the Sanjiang Plain Wetland, and the Songnen Plain Wetland. The distribution of wetlands in other locations tends to be scattered. Due to its extremely rich wetland resources, the HRBC has become an important and key breeding ground and migration stop for cranes. There are 15 kinds of cranes in the world, nine of which can be found in China, among which seven are distributed in the study area. Among these, red-crowned cranes, which are protected as first-class national protected animals, are also widely distributed in the HRBC (Fig. 1b). The population of wild red-crowned cranes in the HRBC is about 280, accounting for more than 10% of the global wild red-crowned cranes. They mainly breed in the Zhalong National Nature Reserve, Xianghai National Nature Reserve, Momoge Nature Reserve, Xingkai Lake Nature Reserve, and many other national nature reserves (Ma and Li, 1990; Xu et al., 1995).

With the development of the social economy in the HRBC, the wetland area has been sharply reduced and the biodiversity has been damaged, bringing great challenges to the survival environment of red-crowned cranes. For example, the Zhalong National Nature Reserve, which is one of the important habitats of red-crowned cranes, has seen its wetland area shrink in the past few decades, with a corresponding decrease in the number of wild red-crowned cranes (Wang et al., 2011; Wang et al., 2017; Yu and Liu, 2018). Meanwhile, in the Sanjiang Plain Wetland, the agricultural land area has increased by nearly 4-fold over the past 60 years, while the wetland area has decreased from 4.43 million hm^2 to 1.51 million hm^2, a loss rate of 0.058 million hm^2 per year (Yi, 2014). The fragmentation of the wetland system has resulted in some wetlands no longer featuring the conditions necessary for red-crowned crane habitation, which has greatly reduced the landscape connectivity of the habitat and seriously affected the spatial distribution of the red-crowned crane (Ma and Jin, 1985; Zhao et al., 2019). Therefore, wetland protection in the HRBC faces numerous difficulties and problems. Wetland protection is no longer limited to the maintenance of the status quo, but now must focus on the restoration and reconstruction of degraded and damaged wetland systems.

2.2. Data sources

The data source of this study is the land use data (30m * 30m) jointly produced by the Institute of geographic sciences and natural resources research, Chinese Academy of Sciences and the Resource and Environment Data Cloud Platform. Based on the interpretation of the acquired Landsat image data and the verification of field investigation, the land use remote sensing images of the Heilongjiang river basin in China in 1980, 1990, 2000, 2005, 2010 and 2015 were extracted. In addition, meteorological data are from the China meteorological science data sharing network (http://data.cma.cn) and the hydrological yearbook of the People's Republic of China, which include precipitation, temperature and so on.

3. Methods

3.1. Analysis of wetland system evolution trend

In this study, based on the migration and habitat conditions of typical migratory birds (i.e., red-crowned cranes), five land use types were selected to constitute the wetland system, namely, river, lake, reservoir, beach, and marsh. Based on the classification and statistics function of the ArcGIS software package, the landscape area change, landscape dynamicity model, and landscape conversion matrix of the wetland system were analyzed and calculated.

3.1.1. Landscape area change

According to the interpreted landscape pattern type data, the areas of different landscape types in any 2 periods were counted and the change of landscape area was calculated. The expression used was:

$U = U_b - U_a$ (1)

where U denotes change in landscape area, km^2;U_a represents the area of some type of landscape in the initial stage, km^2; and U_b represents the area of some type of landscape in the last stage, km^2.

3.1.2. Landscape dynamicity model

The dynamic rate of the wetland landscape and the dynamic rate of the integrated wetland landscape were important indicators when evaluating the dynamic change rate of certain landscape types and regional landscapes during the study period. The formulas for both indicators are as follows (Bai et al., 2013; Ouyang et al., 2018):

$LC = \frac{U_b - U_a}{U_a} \times \frac{1}{T} \times 100\%$ (2)

$LCG = \frac{\sum_{i=1}^{n} LU_{i-j}}{2\sum_{i=1}^{n} LU_i} \times \frac{1}{T} \times 100\%$(3)

where LC denotes the dynamic rate of a certain wetland landscape type; LU_i is the landscape area at the initial stage;LU_{i-j} is the absolute value of the area when the landscape is converted into other landscape types during the research stage; and$T$ is the length of the research stage. If T represents time in years, LC and LCG denote the annual dynamic rates of a particular wetland landscape type and of the entire wetland landscape, respectively.

3.1.3. Landscape conversion matrix

The conversion matrix has been widely adapted to study landscape type change. Conversion matrices can comprehensively and specifically characterize the direction and structural characteristics of various types of landscape changes, and can also be utilized to precisely study the loss and transfer between two types of landscape types in a given area. The conversion matrix can be expressed as follows (Bai et al., 2013; Li and Zeng, 2018):

$S_{\mathrm{ij}} = |$

$$\begin{matrix} S_{11} & amp; S_{12} & amp; \cdots & amp; S_{1n} \\ S_{21} & amp; S_{22} & amp; \cdots & amp; S_{2n} \\ \vdots & amp; \vdots & amp; \vdots & amp; \vdots \\ S_{n1} & amp; S_{n2} & amp; \cdots & amp; S_{\mathrm{nn}} \end{matrix} \quad (4)$$

where S represents the area of a certain landscape type; $n$refers to the wetland landscape type number; and i and j are the landscape types in different periods. The landscape conversion matrix can be employed to obtain information concerning the transformation between different landscape types at the beginning and the end of the study period, which has rich statistical significance.

3.2. Evaluation and regulation of the SSC

The SSC of the wetland system combines the traditional hydrological connectivity with the environmental and ecological functions required to maintain the habitat and migration of migratory birds. The ecological behavior of typical migratory birds, such as their habitat and migration, is analyzed and calculated based on the need for internal wetland functions and wetland connectivity. The SSC fully reflects the health of the entire large-scale wetland system. Based on the analysis of the evolutionary trend of the wetland system, the evaluation and regulation of the wetland system SSC proposed by this research on migratory bird migration primarily consists of four steps: Step 1. Remote sensing image processing; Step 2. Screening for effective habitat; Step 3. Calculation of SSCI; and Step 4. Connectivity evaluation and regulation (Figs. 2 and 3).

Fig. 2 . Flowchart depicting the different methodological steps of the proposed stereoscopic spatial connectivity (SSC) evaluation and regulation.

First, the obtained remote sensing image is interpreted. From these images, the spatial distribution of different land use types in the area is obtained through interpretation methods (Fig. 3a). Based on the habits of the typical migratory birds in the study area, the types of land use suitable for the habitation of these birds are extracted, such as river, lake, reservoir, beach, and marsh. These are then used as basic data for the suitable habitat spatial distribution (Fig. 3b).

Second, the effective habitat is screened based on the spatial distribution of the suitable habitat. Screening for the effective habitat involves two processes. The first is conducting a preliminary screening of the spatial distribution map (Fig. 3b) of the suitable habitat obtained from Step 1. The patches smaller than the minimum area required for typical migratory birds to inhabit are then removed, in order to obtain a preliminary screened effective habitat distribution map (Fig. 3c). The second process divides the entire region into grid squares of appropriate side lengths, and then projects Fig. 3d onto the grid. Each grid square is regarded as the minimum unit, and the suitable habitat area within each grid is calculated cumulatively. The grid squares containing habitat areas smaller than the minimum required for typical migratory birds are eliminated, and the effective habitat distribution map is screened twice (Fig. 3d).

Next, the SSCI of the regional wetland system is calculated. Prior to the calculation, the distance threshold of the patch connectivity within the landscape was preset by considering the single flight capability and migration characteristics of typical migratory birds. The selected effective habitat distribution map was taken as the center, while the preset distance threshold was taken as the expansion radius for effective expansion (Fig. 3e). The "Euclidean distance" calculation method was used in this study, and the distribution formula was:

$$\left[(x_m - x_i)^2 + (y_n - y_j)^2\right]^{\frac{1}{2}} \times D \leq L(5)$$

In this formula, if the projected mesh in the research area is $a*b$,$(x_m,\ y_n)$ represents the position coordinates of the effective water surface mesh particle obtained in step 3, with$1 \leq m \leq a$,$1 \leq n \leq b$; $(x_i,\ y_j)$ represents the position coordinates satisfying the migration grid of typical migratory birds, $1 \leq i \leq a$,$1 \leq j \leq b$; D is the length of the square grid, km^2; and L is the maximum flight distance of typical migratory birds in the target area, km^2.

All of the grid squares that meet Eq. (5) are identified and labeled. By considering factors such as watershed distribution and topography, the disconnected regions with small distribution ranges are eliminated. The maximum connected patches meeting the habitat and migration conditions of the target migratory birds are screened in order to determine the region of the SSC (Fig. 3f). The ratio of the mesh number of the maximum connected patches to the total mesh number of the study area represents the SSC of the regional wetland system. Its expression is:

$\mathrm{SSCI} = \frac{N_{\mathrm{EWS}}}{N} \times 100\%$ (6)

where N_{EWS} (EWS = effective water surface) is the number of effective grid squares contained in the connected region and Nrepresents the total number of grid squares covered by the target research area.

Finally, based on the calculation results, the optimal control measures of the SSC of the regional wetland system are proposed. Combined with the river basin attributes, topography, human activity, and land use status of the study area, the key protected areas in the connected area (Fig. 3g) and the key recovery areas in the unconnected area (Fig. 3h) are proposed under the current conditions, so as to suggest a regional SSC regulation plan. The connectivity before and after regulation is compared, and the feasibility of the scheme is comprehensively considered in order to select and optimize the regulation scheme.

Fig. 3 . Operational steps for the evaluation and regulation of the stereoscopic spatial connectivity (SSC).

4. Results

4.1. Analysis of the wetland system evolutionary trend in the HRBC

The wetland system changes in the HRBC are shown in Fig. 4 and Table 1. From 1980–2015, the wetland system area decreased from 68,617 km^2 to 55,468 km^2, accounting for 6.1% of the total area of the study area, down from 7.5%. Compared with 1980, the area of the wetland system had decreased by 19.2% in 2015, indicating a dynamic rate of -0.5%. Within the wetland system, the area of marsh exhibited the greatest shrinkage, decreasing 12,114 km^2, a change of 25.9% and a dynamic rate of -0.7%. The lake, beach, and river areas all shrank slightly, decreasing 1,088 km^2, 399 km^2, and 96 km^2, respectively. Contrary to these results, the reservoir area displayed continuous growth. From 1980–2015, the reservoir area increased by 549 km^2, an expansion of 30.7%, reflecting the largest dynamic rate of 0.9%.

In terms of time series, the HRBC wetland system area changed more dramatically between 1980 and 2000. During this period, which corresponded to the early stage of China's reform and opening-up, human social activities intensified, and the rate of land reclamation and urbanization increased rapidly. As a result, marsh, lake, beach, and river areas all shrank to a certain extent, decreasing 9,713 km^2, 705 km^2, 207 km^2, and 65 km^2, respectively. Among them, the reductions of marsh and lake areas were significant, reaching -20.8% and -8%, respectively, corresponding to dynamic rates of -1% and -0.4%. At the same time, the reservoir area increased by 13.2%, although since the reservoir area increased by only 237 km^2, its mitigation of the shrinking trend of the entire wetland system had less impact. The proportion of the wetland system to the total study area decreased from 7.5% to 6.4%. From 2000 to 2015, the shrinkage trend of the HRBC wetland system area became relatively slow, and the proportion to the total study area decreased from 6.4% to 6.1%. The shrinkage rate was much lower than that of 1980–2000. Thus, the encroachment rate on the wetland system has slowed down to some extent.

Table 1 Area trends of various types of water bodies from 1980–2015.

Fig. 4 . Area trends of various types of water bodies from 1980–2015.

Fig. 5 shows the spatial change of the wetland system in the HRBC. It can be seen that the distribution range of the wetland system decreased continually from 1980–2015. Within this system, the spatial distribution of the marsh area decreased most noticeably, primarily in the Sanjiang Plain. The spatial distribution of the reservoir increased by a small amount, however, which increased the spatial extent of the wetland system to a certain extent.

Fig. 5 . Spatial distribution trends of various types of water bodies from 1980–2015.

4.2. Transition matrix analysis of the wetland system

The analysis of the conversion among land use types is used to uncover the internal conversion among different land use types. In this study, ArcGIS software was utilized to overlay and analyze the spatial distribution of the wetland system in the HRBC from 1980–2015, thus obtaining the spatial transition matrices (Tables 2–4, and Fig. 6). Tables 2 and 3 show the conversions of various types of land use within the wetland system as well as outside it. As shown in Table 2, from 1980–2015, 17,197 km^2 of the wetland system was converted to various types of land use. The conversion loss of marsh was the largest, reaching 14,949 km^2 and accounting for 86.9% of the total conversion loss area, followed by beach, lake, reservoir, and river areas, with conversion loss areas of 1,047 km^2, 958 km^2, 155 km^2, and 89 km^2, respectively. Among the areas obtained after conversion, agricultural land exhibited the most generation, reaching 13,476 km^2 and accounting for 78.4% of the total converted area. As shown in Table 3, from 1980–2015, 4,049 km^2 of various types of external land use types were converted to the wetland system. Among them, marsh transferred the most area, reaching 2,865 km^2 and accounting for 70.8% of the total converted area, followed by reservoir, beach, lake, and river areas (511 km^2, 402 km^2, 219 km^2, and 51 km^2, respectively). Among the various types of external land use transferred to the wetland system mentioned above, grassland and agricultural land contributed the most, totaling 1,499 km^2 and 1,341 km^2, respectively, and correspondingly accounting for 37.0% and 33.1% of the total transferred area. Table 4 shows the transfer of various types of land use within the wetland system from 1980–2015, with the areas of river, lake, and marsh decreasing, and the areas of reservoir and beach increasing slightly.

Table 2 Reduction of the wetland system area transfer matrix in 2015 compared to 1980.

Table 3 Increase of the wetland system area transfer matrix in 2015 compared to 1980.

Table 4 Internal transfer matrix of the wetland system area in 2015 compared to 1980.

Fig. 6 . Reduced/increased water area distribution in 2015 compared to 1980.

4.3. SSCI evaluation of the wetland system

In accordance with the temporal variation law of the wetland system in the study area, this investigation selected 1980, 2000, and 2015 as the typical years, and chose the red-crowned crane as the target organism for SSC evaluation. Based on the wetland system distribution map extracted in Fig. 5, the SSC evaluation method was employed to remove small patches that did not meet the red-crowned crane's habitat requirements, and the habitat area grid (5 km $\times$ 5 km) was generalized. Centering on the grid of the inhabitable areas, and taking the single-flight capability of a red-crowned crane as a radius of 40 km, the migratory region was expanded, as shown in Fig. 6a (Li et al., 2015; Li et al., 1994). The maximum connected patches (Fig. 6b) were then screened in the migratory region in order to obtain the evaluation results of the SSC of the regional wetland system.

As shown in Table 5, in terms of time scale, the habitable area of red-crowned cranes in the HRBC decreased from 166,950 km^2 to 138,150 km^2 over the period 1980–2015. Thus, the area decreased by 28,800 km^2, a 17.3% reduction. The migratable area shrank drastically from 1980–2000, accounting for 89.5% of the reduction for the entire period. The migration area of the red-crowned cranes in the basin decreased from 450,575 km^2 in 1980 to 414,425 km^2 in 2015, a decrease of 8%. The largest connected patch in the study area decreased from 356,400 km^2 in 1980 to 302,725 km^2 in 2015, a decrease of 15.1%. Finally, it was determined that from 1980–2015, the SSCI of the river basin decreased from 41.3% to 35.1%, a decrease of 15%. The reduction trend was mainly concentrated before 2000, accounting for 96.8% of the overall decrease.

In terms of spatial scale, the spatial distribution of wetland system in HRBC from 1980 to 2018 is shown in Fig.7. The area with the most severe shrinkage of migratory area was concentrated on the Sanjiang Plain. This was mainly due to the further large-scale development of agricultural reclamation on the Sanjiang Plain associated with social and economic development and the increasing demand for grain that began in the 1980s. The farmland development area is more than 20 million mu (Yi, 2014). In addition, the Songnen Plain area is the site of frequent human activities, including cultivation and urbanization, which have also caused damage to the wetland system in the basin, leading to a certain amount of wetland area degradation (Liu et al., 2014; Zhang et al., 2019). As a result of these changes, the suitable habitat areas and migration paths of red-crowned cranes have been largely lost, and measures should be taken to strengthen the protection and restoration of wetlands in the appropriate areas.

Fig. 7 . Stereoscopic connected areas of the wetland system.

Table 5 Stereoscopic connected areas and their associated wetland system index.

5. Discussion

5.1. Cause of the evolutionary trends in the wetland system and stereoscopic spatial connectivity

The SSC changes described in this study were primarily caused by the evolution of the wetland system, which was influenced by both climate change and human activity. Climate change mainly affects the spatial and temporal distribution of the ecological and hydrological processes in wetland system areas on a large scale, and is one of the important driving factors in wetland system change. In particular, temperature and precipitation are 2 important meteorological factors affecting wetland systems (Cui et al., 2019; Cui et al., 2018; Leroux et al., 2017; Liu et al., 2018; Muradyan et al., 2019; Yu et al., 2012). As shown in Fig. 8a and b, by analyzing the meteorological data of 62 national meteorological stations located in the HRBC from 1980–2015, the trends of annual average temperature and precipitation were obtained. The HRBC has been warming since 1980, with the average annual temperature rising at a rate of 0.027°C/year. As the temperature rises, evaporation will increase, and the wetland system will shrink. In addition, the average annual precipitation in the HRBC has decreased slightly over the past 35 years. Since precipitation is an important water source for wetlands, the changing precipitation trend will also affect the spatial and temporal distribution of wetland systems. It is worth noting that from 2000–2015, the average annual precipitation in the study area increased significantly, and the wetland system shrinkage gradually slowed.

Fig. 8 . Trends of various driving factors from 1980–2015.

The influence of human activity, however, remains the most important factor in wetland system shrinkage in the study area (Chen et al., 2019; Fluet-Chouinard et al., 2015; Hudon et al., 2018; Zhang et al., 2019). Fig. 8c and d show that both agricultural land and construction land in the Heilongjiang Basin are increasing significantly. Of these, agricultural land increased significantly, at the rate of 1,292.79 km^2/year, replacing large sections of the original wetland system. Moreover, most of the expansion occurred before 2000, with the increase after 2000 being relatively small, which was basically consistent with the shrinkage trend of the wetland system. For example, some researchers discovered that the area of the global wetland ecosystem exhibited a decreasing trend from 1977–2011 (Costanza et al., 2014). At the same time, the shrinkage of the wetland system in the HRBC was mainly due to the change of land use in the Sanjiang Plain area, where the lost area of the wetland system was primarily converted into agricultural land, which also led to the decrease of ecosystem service value (Yan and Zhang, 2019). In addition, improved wetland protection policy also has an important impact on wetland systems. Since 2000, increasing attention has been paid to the degradation of wetland systems, and a large number of national nature reserves have been improved. The shrinkage trend of the wetland system in the HRBC has been effectively alleviated by strengthening the protection of wetland systems (Fu et al., 2015; Liu et al., 2011). In summary, climate change and human activity have contributed to the shrinking of the wetland system in the HRBC over the past 35 years, with large-scale agricultural reclamation and development being the main driving factors behind this reduction.

5.2. SSC regulation scheme for wetland systems and feasibility analysis

In this study, 2015 was selected as the current year and a "double-key area" approach including both key protected areas and key recovery areas was proposed in order to improve the SSC of the wetland system in the river basin. The key protected areas are the key areas that should be protected in order to maintain the existing connected system. Fig. 9a shows the selected key protected areas. The following 2 factors are considered during screening: (1) In terms of ecological function, the key protected areas are the key channels connecting suitable habitats of red-crowned cranes. They provide an important guarantee for the wetland system SSC; (2) In terms of the possibility of being affected, these areas experience frequent human activity and the wetland system is relatively fragile. In order to ensure that the connectivity under current conditions is not destroyed, protection efforts should be enhanced.

The key restoration area is based on the existing connectivity system. It restores some areas that currently do not meet the red-crowned crane's habitat requirements, and can greatly improve the overall connectivity of the river basin wetland system. Fig. 9b–d shows the selected recovery areas. During the process of screening the key recovery areas, the following 3 scenarios were developed based on feasibility, from high to low.

Scenario (a): High feasibility. At the key points that can significantly increase the connected area, expand the existing small water areas that do not meet the habitat conditions of the red-crowned crane, so that the restored waters meet the habitat conditions. The key recovery areas and recovery results of scenario (a) are shown in Table 6, Fig. 9b, and Fig. 10b. Through the ecological restoration of small water areas, the connectivity of the Sanjiang Plain can be restored. The connected area in this region would be close its 1980 coverage, and connected area could be added to the southeast of the study area. It was calculated that the SSCI energy would increase to 38.7%, and the number of connected paths within the wetland system would increase from 60 under the current conditions to 70 after restoration.

Scenario (b): Medium feasibility. Based on scenario (a), the key points of the red-crowned crane migration path would be selected, and the dryland, woodland, grassland, and other transformable land use types would be restored to wetlands that meet the red-crowned crane's habitat. The key recovery areas and recovery results of scenario (b) are shown in Table 6, Fig. 9c, and Fig. 10c. Through the transformation of land use types, the SSCI would increase to 40.6%, basically returning to the connectivity level of the basin in 1980. The regulation scheme of scenario (b) would add generalization routes in the study area, increasing the total number of generalization routes to 116, which is 1.93 times the pre-regulation total.

Scenario (c): Low feasibility. On the basis of scenario (b), the Songhua River Basin would be connected to the Heilongjiang Mainstream Basin and the Ergun River Basin through recovery measures, which would greatly improve the overall connectivity of the wetland system in the study area. The key recovery areas and recovery results of scenario (c) are shown in Table 6, Fig. 9d, and Fig. 10d. The SSCI would increase to 47.6%, which is 1.36 times its 2015 value. The total number of generalization route would reach 131, which is 2.18 times the pre-regulation total.

Based on the results of the above three scenarios and the feasibility of the schemes, the suggestion of this study is to quickly give priority to scenario (a) and then to scenario (b). Through the regulation methods of scenarios (a) and (b), the wetland system area and SSCI for the red-crowned crane habitat would effectively improve, and the conditions for the habitat and migration of red-crowned cranes would be restored to 1980 levels. After the number of red-crowned cranes in the region has increased significantly, consider implementing scenario (c) via human intervention. Through the regulation mode of scenario (c), the habitat area and migration area of the red-crowned crane could be greatly expanded.

Table 6 Regulated stereoscopic connected areas and their associated wetland system index.

Fig. 9 . Regulated stereoscopic connected areas of the wetland system.

Fig. 10 . Regulated generalized migration routes of the wetland system.

6. Conclusions

This study summarized the evolution of the wetland system in the Heilongjiang River Basin over the past 35 years. Through the establishment of SSC evaluation and regulation methods for the habitat and migration requirements of typical migratory birds (in this case, red-crowned cranes), the potential laws of the ecological hydrological process and SSCI of the wetland system in the study area are revealed. The results indicate that the wetland system in the HRBC was seriously destroyed from 1980–2015. The wetland area decreased by 19.2% within these 35 years, during which the increase of agriculture land was the major driving factor leading to the reduction of wetland in the study area. During the same period, the SSCI of the wetland system in the study area also gradually decreased, from 41.3% in 1980 to 35.1% in 2015, which compressed the habitat area and migration path of red-crowned cranes. Based on these findings, five key protected areas under the current connectivity system of the wetland system in the study area were screened, and three progressive restoration scenarios were proposed based on feasibility level, which could greatly improve the SSCI and the number of generalization routes of the wetland system in the basin.

Aspects of this topic still require further study. For example, in terms of the requirements of the habitat and migration of migratory birds, this investigation only considered wetland size as the evaluation criterion, which is not comprehensive enough. Other factors such as water depth, vegetation distribution, and distance from human activities in the region also need to be analyzed in future studies in order to more accurately evaluate the SSC in regional wetland systems and to establish comprehensive regulation measures.

Acknowledgements

This work was supported by the National Key Research and Development Program of China [grant numbers 2017YFC0404503, 2016YFC0401302]; the National Natural Science Foundation of China [grant number 51625904]; and the Basic Scientific Research Expense Project of the China Institute of Water Resources and Hydropower Research [grant number WR0145B522017].

Data Availability Statement

The data that support the findings of this study are available from the corresponding author upon reasonable request.

Conflict of Interest Statement

Conflict of Interest – None.

References

Acreman, M.C., Fisher, J., Stratford, C.J., Mould, D.J., Mountford, J.O., 2007. Hydrological science and wetland restoration: some case studies from Europe. Hydrol. Earth Syst. Sci. 11, 158–169. https://dx.doi.org/10.5194/hess-11-158-2007.

Ameli, A.A., Creed, I.F., 2017. Quantifying hydrologic connectivity of wetlands to surface water systems. Hydrol. Earth Syst. Sci. 21, 1791–1808. https://dx.doi.org/10.5194/hess-21-1791-2017.

Bai, J.H., Lu, Q.Q., Wang, J.J., Zhao, Q.Q., Ouyang, H., Deng, W., Li, A.N., 2013. Landscape pattern evolution processes of alpine wetlands and their driving factors in the Zoige Plateau of China. J. Mt. Sci. 10, 54–67. https://dx.doi.org/10.1007/s11629-013-2572-1.

Chen, W., Cao, C., Liu, D., Tian, R., Wu, C., Wang, Y., Qian, Y., Ma, G., Bao, D., 2019. An evaluating system for wetland ecological health: case study on nineteen major wetlands in Beijing-Tianjin-Hebei region, China. Sci. Total Environ. 666, 1080–1088. https://dx.doi.org/10.1016/j.scitotenv.2019.02.325.

Cook, B.J., Hauer, F.R., 2007. Effects of hydrologic connectivity on water chemistry, soils, and vegetation structure and function in an intermontane depressional wetland landscape. Wetlands 27, 719–738. https://dx.doi.org/10.1672/0277-5212(2007)27[719:eohcow]2.0.co;2.

Costanza, R., d'Arge, R., de Groot, R., Farber, S., Grasso, M., Hannon, B., Limburg, K., Naeem, S., O'Neill, R.V., Paruelo, J., Raskin, R.G., Sutton, P., van den Belt, M., 1997. The value of the world's ecosystem services and natural capital. Nature 387, 253–260. https://dx.doi.org/10.1038/387253a0.

Costanza, R., de Groot, R., Sutton, P., van der Ploeg, S., Anderson, S.J., Kubiszewski, I., Farber, S., Turner, R.K., 2014. Changes in the global value of ecosystem services. Glob. Environ. Change 26, 152–158. https://dx.doi.org/10.1016/j.gloenvcha.2014.04.002.

Cui, L., Wang, L., Qu, S., Singh, R.P., Lai, Z., Yao, R., 2019. Spatiotemporal extremes of temperature and precipitation during 1960–2015 in the Yangtze River Basin (China) and impacts on vegetation dynamics. Theor. Appl. Climatol. 136, 675–692. https://dx.doi.org/10.1007/s00704-018-2519-0.

Cui, L., Wang, L., Singh, R.P., Lai, Z., Jiang, L., Yao, R., 2018. Association analysis between spatiotemporal variation of vegetation greenness and precipitation/temperature in the Yangtze River Basin (China). Environ. Sci. Pollut. Res. Int. 25, 21867–21878. https://dx.doi.org/10.1007/s11356-018-2340-4.

Dong, L., Zhang, G., 2013. The dynamic evolvement and hydrological driving factors of marsh in Nenjiang River basin. Shuikexue Jinzhan 24, 177–183. https://dx.doi.org/10.14042/j.cnki.32.1309.2013.02.011.

Evenson, G.R., Golden, H.E., Lane, C.R., D'Amico, E., 2015. Geographically isolated wetlands and watershed hydrology: a modified model analysis. J. Hydrol. 529, 240–256. https://dx.doi.org/10.1016/j.jhydrol.2015.07.039.

Ferone, J.M., Devito, K.J., 2004. Shallow groundwater–surface water interactions in pond–peatland complexes along a Boreal Plains topographic gradient. J. Hydrol. 292, 75–95. https://dx.doi.org/10.1016/j.jhydrol.2003.12.032.

Fluet-Chouinard, E., Lehner, B., Rebelo, L.M., Papa, F., Hamilton, S.K., 2015. Development of a global inundation map at high spatial resolution from topographic downscaling of coarse-scale remote sensing data. Remote Sens. Environ. 158, 348–361. https://dx.doi.org/10.1016/j.rse.2014.10.015.

Fu, L., Kong, S., Zong, C., Ma, J., 2015. The difference of spatial distribution of wetland natrue reserves and wetland parks in China. Shidi Kexue 13, 356–363. https://dx.doi.org/10.13248/j.cnki.wetlandsci.2015.03.014.

Hudon, C., Jean, M., Létourneau, G., 2018. Temporal (1970–2016) changes in human pressures and wetland response in the St. Lawrence River (Québec, Canada). Sci. Total Environ. 643, 1137–1151. https://dx.doi.org/10.1016/j.scitotenv.2018.06.080.

Januchowski-Hartley, S.R., McIntyre, P.B., Diebel, M., Doran, P.J., Infante, D.M., Joseph, C., Allan, J.D., 2013. Restoring aquatic ecosystem connectivity requires expanding inventories of both dams and road crossings. Front. Ecol. Environ. 11, 211–217. https://dx.doi.org/10.1890/120168.

Jaramillo, F., Brown, I., Castellazzi, P., Espinosa, L., Guittard, A., Hong, S.H., Rivera-Monroy, V.H., Wdowinski, S., 2018. Assessment of hydrologic connectivity in an ungauged wetland with InSAR observations. Environ. Res. Lett. 13, 024003. https://dx.doi.org/10.1088/1748-9326/aa9d23.

Karim, F., Kinsey-Henderson, A., Wallace, J., Arthington, A.H., Pearson, R.G., 2012. Modelling wetland connectivity during overbank flooding in a tropical floodplain in north Queensland, Australia. Hydrol. Process. 26, 2710–2723. https://dx.doi.org/10.1002/hyp.8364.

Karim, F., Kinsey-Henderson, A., Wallace, J., Godfrey, P., Arthington, A.H., Pearson, R.G., 2014. Modelling hydrological connectivity of tropical floodplain wetlands via a combined natural and artificial stream network. Hydrol. Process. 28, 5696–5710. https://dx.doi.org/10.1002/hyp.10065.

Karim, F., Petheram, C., Marvanek, S., Ticehurst, C., Wallace, J., Hasan, M., 2016. Impact of climate change on floodplain inundation and hydrological connectivity between wetlands and rivers in a tropical river catchment. Hydrol. Process. 30, 1574–1593. https://dx.doi.org/10.1002/hyp.10714.

Leibowitz, S.G., Vining, K.C., 2003. Temporal connectivity in a prairie pothole complex. Wetlands 23, 13–25. https://dx.doi.org/10.1672/0277-5212(2003)023[0013:tciapp]2.0.co;2.

Leroux, L., Bégué, A., Lo Seen, D., Jolivot, A., Kayitakire, F., 2017. Driving forces of recent vegetation changes in the Sahel: lessons learned from regional and local level analyses. Remote Sens. Environ. 191, 38–54. https://dx.doi.org/10.1016/j.rse.2017.01.014.

Li, C., Zeng, H., 2018. Research on land use change in Longchuan River Basin based on transfer matrix. Renmin Changjiang 49, 39–44. https://dx.doi.org/10.16232/j.cnki.1001-4179.2018.17.007.

Li, S., Ma, J., Wang, W., Du, W., 2015. Behavoiral rhythm research of the Grus japonensis on Zhalong Reserve during the fall-migrating season. Nongbei Nongye Daxue Xuebao 46, 62–69. https://dx.doi.org/10.19720/j.cnki.issn.1005-9369.2015.07.010.

Li, W., Zhao, H., Wang, J., Chen, S., Gao, Q., Zhang, L., 1994. Birds migration in Xingkai Lake area in autumn. Heilongjiang Bayi Nongken Daxue Xuebao 7, 109–110.

Liu, J., Zhao, D., Tian, X., Zhao, L., Liu, J., 2014. Landscape pattern dynamics and driving forces analysis in the Sanjiang Plain from 1954 to 2010. Shengtai Xuebao 34, 3234–3244. https://dx.doi.org/10.5846/stxb201306101639.

Liu, P., Guan, L., Lv, C., Zhang, M.X., Lei, G.C., 2011. Technical characteristics and application prospects of achievements of the second national wetland investigation. Shidi Kexue 9, 284–289. https://dx.doi.org/10.13248/j.cnki.wetlandsci.2011.03.007.

Liu, Z., Liu, Y., Li, Y., 2018. Anthropogenic contributions dominate trends of vegetation cover change over the farming-pastoral ecotone of northern China. Ecol. Indic. 95, 370–378. https://dx.doi.org/10.1016/j.ecolind.2018.07.063.

Ma, Y., Jin, L., 1985. The population distribution of red-crowned cranes in Sanjiang Plain. Guotu Yu Ziran Ziyuan Yanjiu 1985, 38–46.

Ma, Y., Li, X., 1990. The status of red-crowned crane resources in China. Guotu Yu Ziran Ziyuan Yanjiu 1990, 62–64.

McDonough, O.T., Lang, M.W., Hosen, J.D., Palmer, M.A., 2015. Surface hydrologic connectivity between Delmarva bay wetlands and nearby streams along a gradient of agricultural alteration. Wetlands 35, 41–53. https://dx.doi.org/10.1007/s13157-014-0591-5.

Muradyan, V., Tepanosyan, G., Asmaryan, S., Saghatelyan, A., Dell'Acqua, F., 2019. Relationships between NDVI and climatic factors in mountain ecosystems: a case study of Armenia. Remote Sens. Appl. Soc. Environ. 14, 158–169. https://dx.doi.org/10.1016/j.rsase.2019.03.004.

Niu, Z., Zhang, H., Wang, X., Yao, W., Zhou, D., Zhao, K., Zhao, H., Li, N., Huang, H., Li, C., Yang, J., Liu, C., Liu, S., Wang, L., Li, Z., Yang, Z., Qiao, F., Zheng, Y., Chen, Y., Sheng, Y., Gao, X., Zhu, W., Wang, W., Wang, H., Weng, Y., Zhuang, D., Liu, J., Luo, Z., Cheng, X., Guo, Z., Gong, P., 2012. Mapping wetland changes in China between 1978 and 2008. Chin. Sci. Bull. 57, 2813–2823. https://dx.doi.org/10.1007/s11434-012-5093-3.

Ouyang, N., Li, G., Cui, L., Liao, H., 2018. Main features and problems of modern evolution process of coastal wetlands in north Jiangsu, China. J. Indian Soc. Remote Sens. 46, 655–666.

https://dx.doi.org/10.1007/s12524-017-0741-3.

Poff, N.L., Zimmerman, J.K.H., 2010. Ecological responses to altered flow regimes: a literature review to inform the science and management of environmental flows. Freshw. Biol. 55, 194–205. https://dx.doi.org/10.1111/j.1365-2427.2009.02272.x.

Richter, B.D., Baumgartner, J.V., Powell, J., Braun, D.P., 1996. A method for assessing hydrologic alteration within ecosystems. Conserv. Biol. 10, 1163–1174. https://dx.doi.org/10.1046/j.1523-1739.1996.10041163.x.

Rivers-Moore, N., Mantel, S., Ramulifo, P., Dallas, H., 2016. A disconnectivity index for improving choices in managing protected areas for rivers. Aquat. Conserv. 26, 29–38. https://dx.doi.org/10.1002/aqc.2661.

Wang, W., Gao, Z., Li, C., Pang, S., Ma, J., Xu, J., Zhang, X., 2011. Investigations of population size and conservation measures for red-crowned crane in Zhalong Natural Reserve. Yesheng Dongwu 32, 80–82. https://dx.doi.org/10.3969/j.issn.1000-0127.2011.02.006.

Wang, Z., Xu, H., Xu, W., Lin, J., Liu, X., Li, Z., Zhu, J., 2017. Distribution dynamics of red-crowned crane population in Zhalong Wetland by the point pattern analysis. Linye Kexue 53, 168–174. https://dx.doi.org/10.11707/j.1001-7488.20171019.

Wohl, E., Brierley, G., Cadol, D., Coulthard, T.J., Covino, T., Fryirs, K.A., Grant, G., Hilton, R.G., Lane, S.N., Magilligan, F.J., Meitzen, K.M., Passalacqua, P., Poeppl, R.E., Rathburn, S.L., Sklar, L.S., 2019. Connectivity as an emergent property of geomorphic systems. Earth Surf. Process. Landf. 44, 4–26. https://dx.doi.org/10.1002/esp.4434.

Xu, J., Su, L., Zhou, X., Fu, J., You, Z., 1995. Research on the environment and migration of cranes. Yesheng Dongwu 1995, 18–22.

Yan, F., Zhang, S., 2019. Ecosystem service decline in response to wetland loss in the Sanjiang Plain, Northeast China. Ecol. Eng. 130, 117–121. https://dx.doi.org/10.1016/j.ecoleng.2019.02.009.

Yi, B., 2014. Land development and sustainable development of regional ecological environment in the Sanjiang Plain in the past 100 years. Shehui Kexue Zhanxian 2014, 109–114.

Yu, C., Liu, D., 2018. Spatiotemporal evolution of land cover types and response to climate change in Zhalong Wetland. Shengtai Huanjing Xuebao 27, 2117–2126. https://dx.doi.org/10.16258/j.cnki.1674-5906.2018.11.019.

Yu, L.L., Xia, Z.Q., Cai, T., Guo, L.D., 2012. Variations of temperature, precipitation, and extreme events in Heilongjiang River. Procedia Eng. 28, 326–330. https://dx.doi.org/10.1016/j.proeng.2012.01.727.

Zedler, J.B., 2003. Wetlands at your service: reducing impacts of agriculture at the watershed scale. Front. Ecol. Environ. 1, 65–72. https://dx.doi.org/10.1890/1540-9295(2003)001[0065:waysri]2.0.co;2.

Zedler, J.B., Kercher, S., 2005. Wetland resources: status, trends, ecosystem services, and restorability. Annu. Rev. Environ. Resour. 30, 39–74. https://dx.doi.org/10.1146/annurev.energy.30.050504.144248.

Zhang, F., Yushanjiang, A., Jing, Y., 2019. Assessing and predicting changes of the ecosystem service values based on land use/cover change in Ebinur Lake Wetland National Nature Reserve, Xinjiang, China. Sci. Total Environ. 656, 1133–1144. https://dx.doi.org/10.1016/j.scitotenv.2018.11.444.

Zhang, G., Wu, Y., Wu, Y., Liu, X., 2018. A review of reserch on wetland ecohydrology. Shuikexue Jinzhan 29, 737–749. https://dx.doi.org/10.14042/j.cnki.32.1309.2018.05.014.

Zhang, G.X., Yin, X.R., Feng, X.Q., 2008. Review of the issues related to wetland hydrology reserch. Shidi Kexue 6, 105–115.

Zhao, W.J., Xue, Z.S., Wang, Q.B., Yang, M.Y., Sun, K.J., 2019. Effects of land use types on the diversity of migratory birds in spring in Sanjiang Plain based on 3S technologies. Shidi Kexue Yu Guanli 15, 44–48. https://dx.doi.org/10.3969/j.issn.1673-3290.2019.03.10.

Figure list

Fig. 1 . (a) Map of study area and (b) Red-crowned crane's migration route.

Fig. 2 . Flowchart depicting the different methodological steps of the proposed stereoscopic spatial connectivity (SSC) evaluation and regulation.

Fig. 3 . Operational steps for the evaluation and regulation of the stereoscopic spatial connectivity (SSC).

Fig. 4 . Area trends of various types of water bodies from 1980–2015.

Fig. 5 . Spatial distribution trends of various types of water bodies from 1980–2015.

Fig. 6 . Reduced/increased water area distribution in 2015 compared to 1980.

Fig. 7 . Stereoscopic connected areas of the wetland system.

Fig. 8 . Trends of various driving factors from 1980–2015.

Fig. 9 . Regulated stereoscopic connected areas of the wetland system.

Fig. 10 . Regulated generalized migration routes of the wetland system.

Table list

Table 1 Area trends of various types of water bodies from 1980–2015.

Table 2 Reduction of the wetland system area transfer matrix in 2015 compared to 1980.

Table 3 Increase of the wetland system area transfer matrix in 2015 compared to 1980.

Table 4 Internal transfer matrix of the wetland system area in 2015 compared to 1980.

Table 5 Stereoscopic connected areas and their associated wetland system index.

Table 6 Regulated stereoscopic connected areas and their associated wetland system index.

Hosted file

`Tables.docx` available at https://authorea.com/users/323423/articles/452105-an-evaluation-and-regulation-method-for-stereoscopic-spatial-connectivity-of-a-wetland-system-based-on-hydrological-change-a-case-study-of-the-heilongjiang-river-basin-in-china

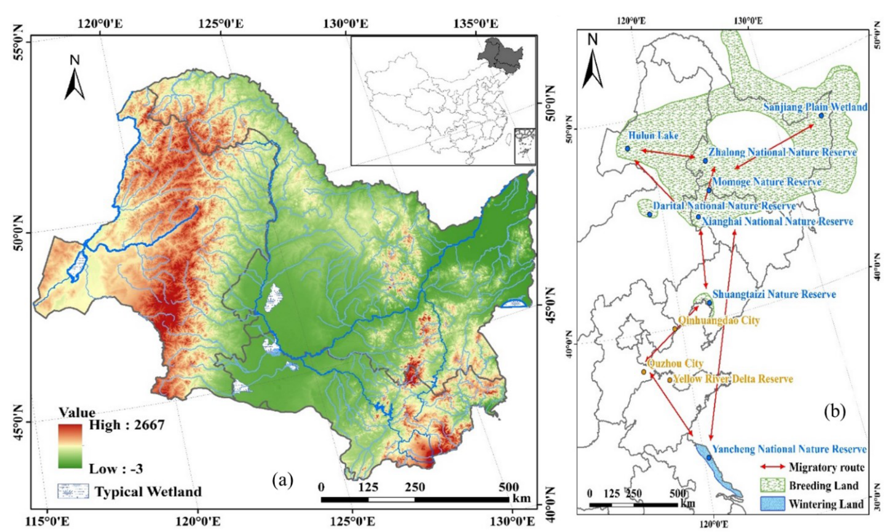

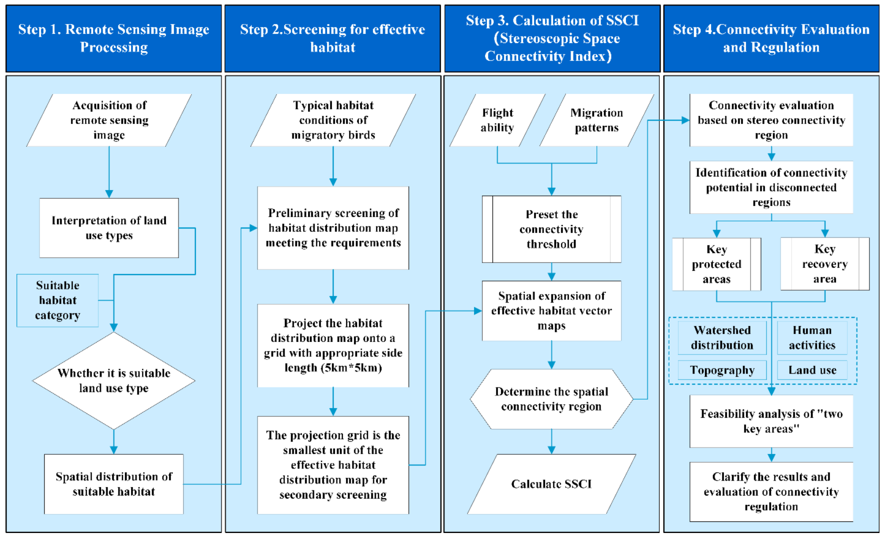
Step 1. Remote Sensing Image Processing
Step 2.Screening for effective habitat
Step 3. Calculation of SSCI (Stereoscopic Space Connectivity Index)
Step 4.Connectivity Evaluation and Regulation
Acquisition of remote sensing image
Interpretation of land use types
Suitable habitat category
Whether it is suitable land use type
Spatial distribution of suitable habitat
Typical habitat conditions of migratory birds
Preliminary screening of habitat distribution map meeting the requirements
Project the habitat distribution map onto a grid with appropriate side length (5km*5km)
The projection grid is the smallest unit of the effective habitat distribution map for secondary screening
Flight ability
Migration patterns
Preset the connectivity threshold
Spatial expansion of effective habitat vector maps
Determine the spatial connectivity region
Calculate SSCI
Connectivity evaluation based on stereo connectivity region
Identification of connectivity potential in disconnected regions
Key protected areas
Key recovery area
Watershed distribution
Human activities
Topography
Land use
Feasibility analysis of "two key areas"
Clarify the results and evaluation of connectivity regulation

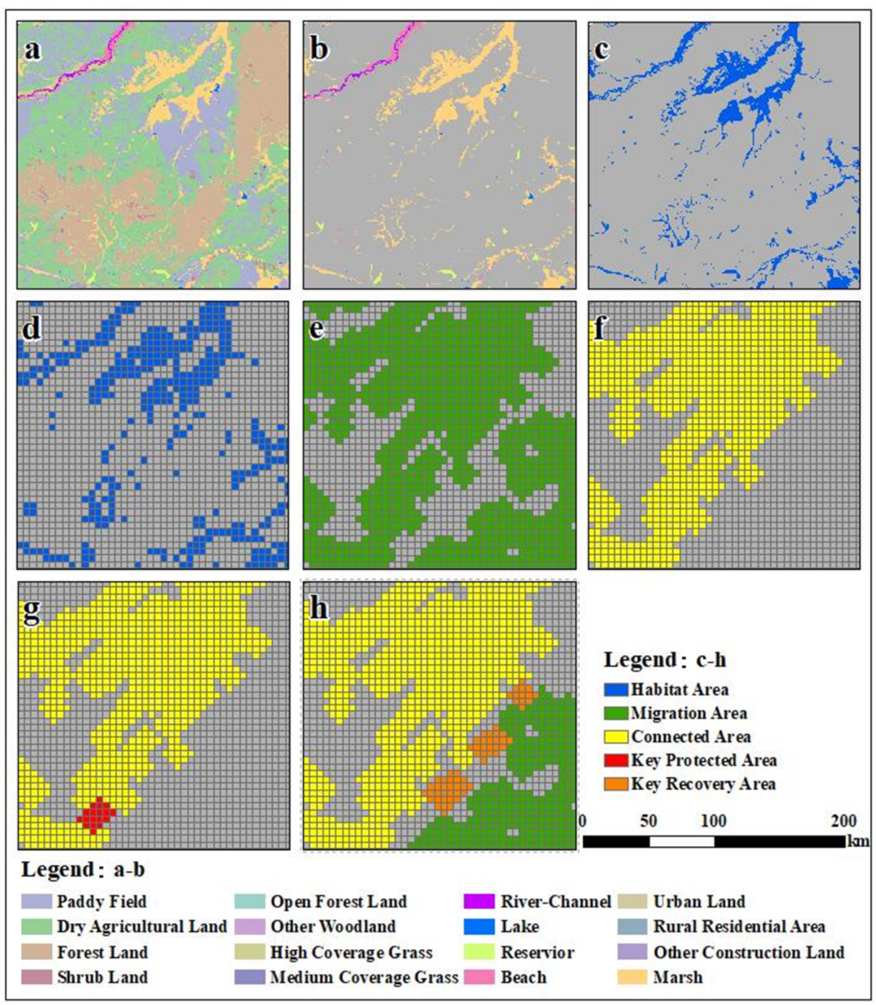
a
b
c
d
e
f
g
h
Legend: c-h
Habitat Area
Migration Area
Connected Area
Key Protected Area
Key Recovery Area
0 50 100 200
km
Legend: a-b
Paddy Field
Dry Agricultural Land
Forest Land
Shrub Land
Open Forest Land
Other Woodland
High Coverage Grass
Medium Coverage Grass
River-Channel
Lake
Reservior
Beach
Urban Land
Rural Residential Area
Other Construction Land
Marsh

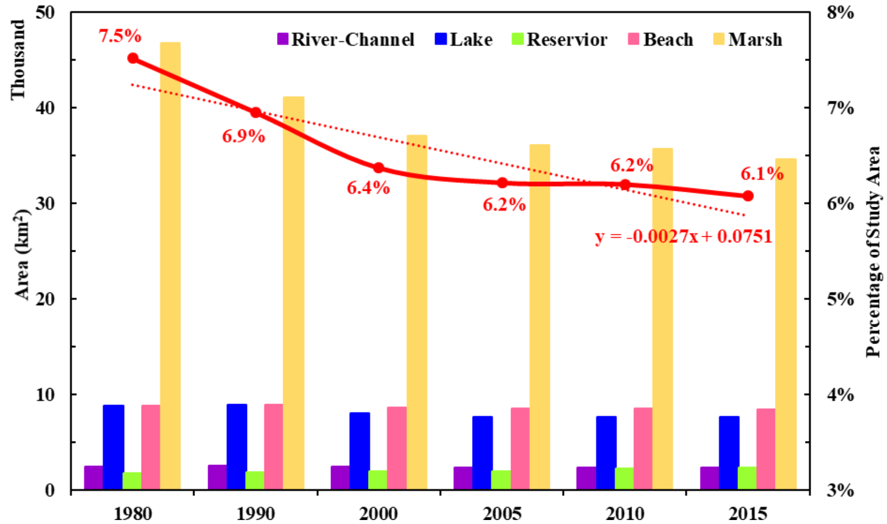
River-Channel
Lake
Reservior
Beach
Marsh
Thousand
Area (km²)
Percentage of Study Area
7.5%
6.9%
6.4%
6.2%
6.2%
6.1%
y = -0.0027x + 0.0751
50
40
30
20
10
0
8%
7%
6%
5%
4%
3%
1980
1990
2000
2005
2010
2015

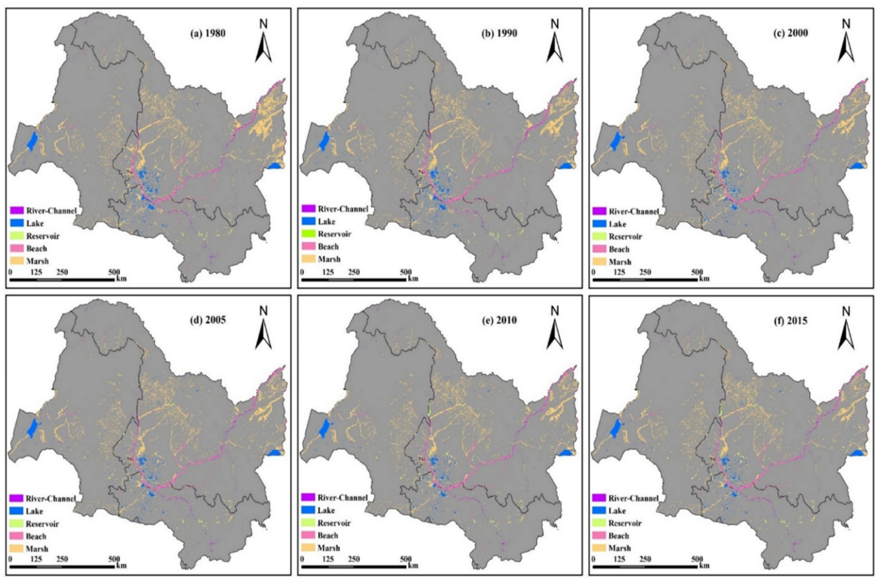
(a) 1980
(b) 1990
(c) 2000
(d) 2005
(e) 2010
(f) 2015
N
River-Channel
Lake
Reservoir
Beach
Marsh
0 125 250 500 km

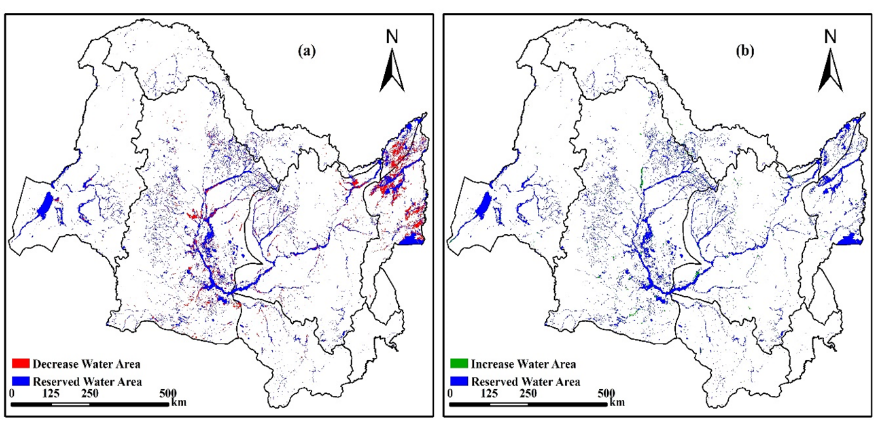
(a)
(b)
N
Decrease Water Area
Reserved Water Area
Increase Water Area
0 125 250 500 km

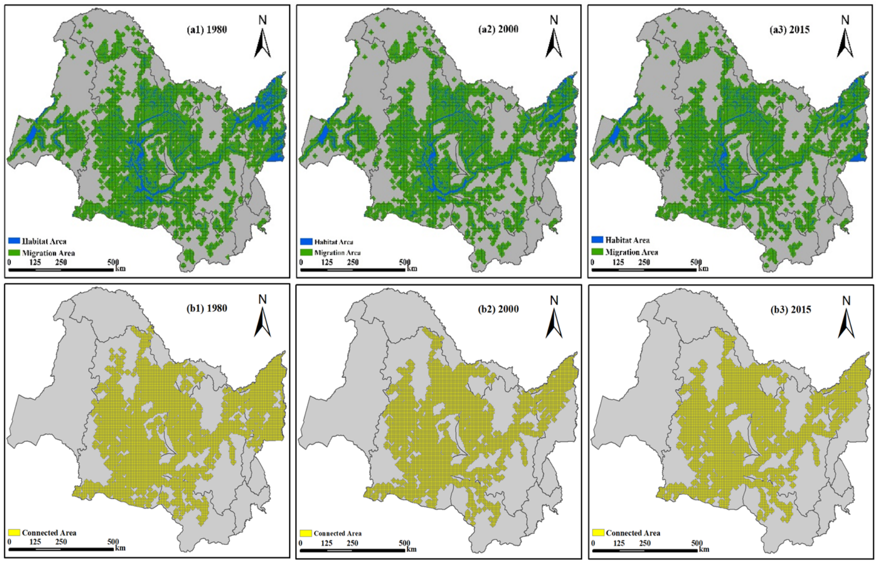

(a1) 1980
(a2) 2000
(a3) 2015
(b1) 1980
(b2) 2000
(b3) 2015
N
Habitat Area
Migration Area
Connected Area
0 125 250 500 km

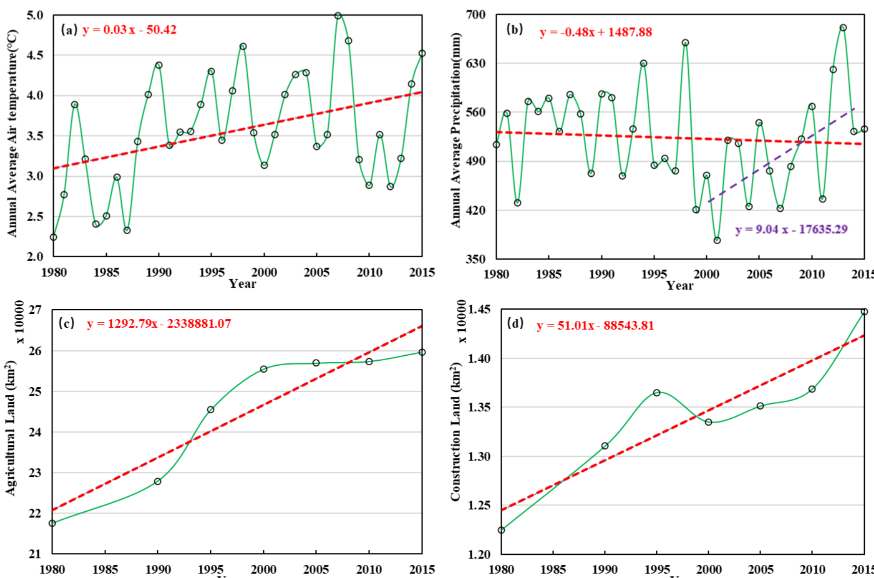

(a) y = 0.03x - 50.42
Annual Average Air temperature(℃)
(b) y = -0.48x + 1487.88
y = 9.04 x - 17635.29
Annual Average Precipitation(mm)
(c) y = 1292.79x - 2338881.07
Agricultural Land (km²) x 10000
(d) y = 51.01x - 88543.81
Construction Land (km²) x 10000
Year

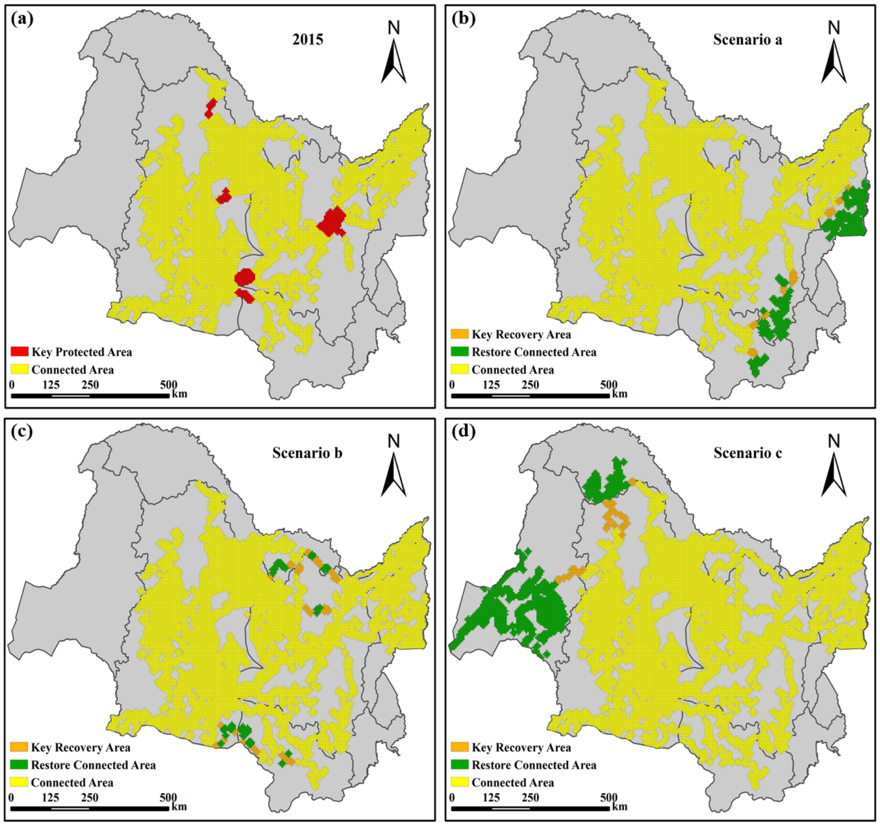
(a)
2015
N
Key Protected Area
Connected Area
0 125 250 500 km
(b)
Scenario a
N
Key Recovery Area
Restore Connected Area
Connected Area
0 125 250 500 km
(c)
Scenario b
N
Key Recovery Area
Restore Connected Area
Connected Area
0 125 250 500 km
(d)
Scenario c
N
Key Recovery Area
Restore Connected Area
Connected Area
0 125 250 500 km

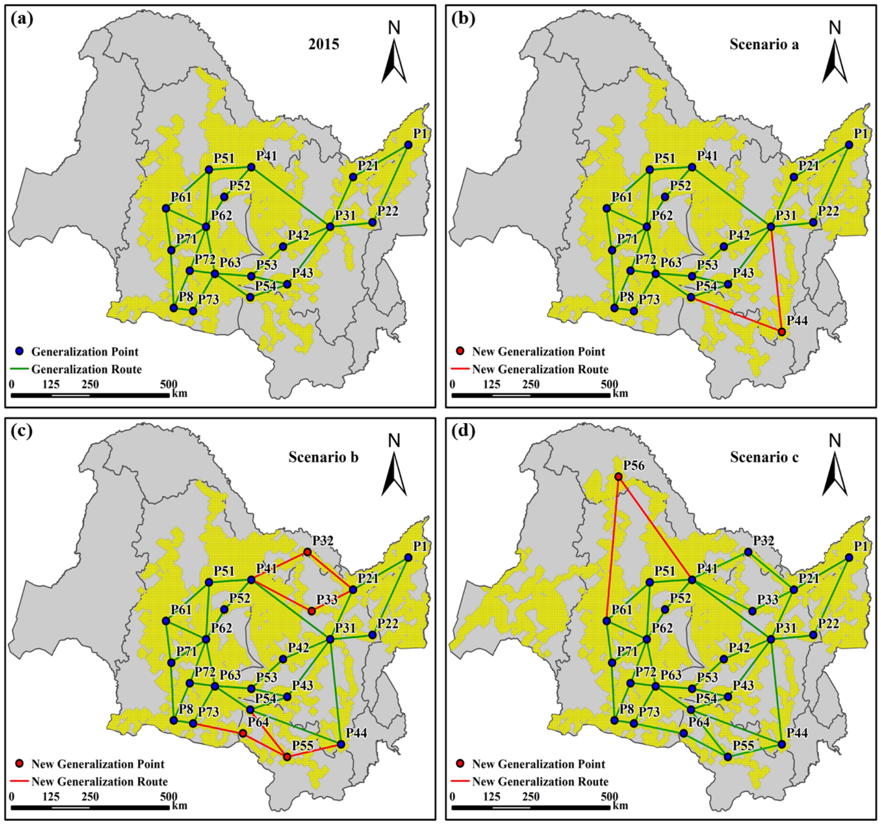
(a)
2015
N
P1
P21
P22
P31
P41
P42
P43
P51
P52
P53
P54
P61
P62
P63
P71
P72
P73
P8
Generalization Point
Generalization Route
0 125 250 500 km
(b)
Scenario a
N
P44
New Generalization Point
New Generalization Route
0 125 250 500 km
(c)
Scenario b
N
P32
P33
P64
P55
P44
New Generalization Point
New Generalization Route
0 125 250 500 km
(d)
Scenario c
N
P56
P32
P33
P64
P55
P44
New Generalization Point
New Generalization Route
0 125 250 500 km